Thermodynamics of the complexation of curium(III) with chloride in alkali and alkali earth metal solutions at elevated temperatures

Carsten Koke [a,b,*], Andrej Skerencak-Frech [b], Petra J. Panak [a,b]

[a] Physikalisch-Chemisches Institut, Ruprecht-Karls-Universität Heidelberg, Im Neuenheimer Feld 253, Heidelberg 69120, Germany
[b] Institut für Nukleare Entsorgung, Karlsruher Institut für Technologie, P.O. Box 3640, Karlsruhe 76021, Germany

ARTICLE INFO

Article history:
Received 4 June 2018
Received in revised form 9 October 2018
Accepted 29 October 2018
Available online 30 October 2018

ABSTRACT

The complexation of trivalent curium (Cm(III)) with chloride up to its respective saturation concentration is studied in dependency of the chloride bearing electrolyte (LiCl, NaCl, $MgCl_2$, $CaCl_2$) in the temperature range of 25 200 °C by time resolved laser fluorescence spectroscopy (TRLFS). At low chloride concentrations and temperatures the Cm(III) aquo ion dominates the species distribution. However, at both elevated chloride concentrations and temperatures speciation is dominated by $CmCl^{2+}$(aq) and $CmCl_2^+$(aq), and significant molar fractions are even contributed by $CmCl_3$ (aq) and $CmCl_4$(aq). Conditional stability constants log $\beta'_n(t)$ are determined and extrapolated to the thermodynamic reference state using the specific ion interaction theory (SIT). Modeling results in standard stability constants log $\beta^\circ_2(t)$ with slight deviation with respect to the valency of the electrolyte. As a result, an average value of log β°_2(25 °C) (1.16 ± 0.10) is derived for the formation of $CmCl_2^+$. The complexation is found to be both endothermic as well as entropy driven with $\Delta_r H^\circ$ (60.5 ± 1.5) kJ mol $^{-1}$, and $\Delta_r S^\circ$ (180.7 ± 3.9) J mol $^{-1}$ K $^{-1}$.

1. Introduction

Nuclear energy is used in about 440 commercial power plants providing roughly 10% of the world's civil electricity [1,2]. However, safe disposal of the nuclear waste is still a focus of attention regarding both fundamental and applied aspects. As actinides are generated through neutron capture, nuclear fuels contain various long lived nuclides (e.g. ^{239}Pu, $t_{1/2}$ = 2.41 10^4 a). The waste has to be safely excluded from the biosphere for time scales of at least 10^6 years. The generally pursued strategy is disposal in deep geological repositories, located in salt, clay, or crystalline rock formations [3,4]. To this end, thermodynamic data of radioactive elements is mandatory for a geochemical model describing the migration behavior of radionuclides in deep rock formations. Given a repository based in rock salt, highly corrosive brines of high ionic strengths I are to be expected in case of water intrusion. As chloride is the most abundant inorganic ligand in salt rock repositories, its weak complexation tendency is easily mitigated by its high concentration in the resulting brine. While thermodynamic data for actinides in their most relevant oxidation states is abundant in various databases, most of the data is restricted to ambient conditions [5,6]. However, near field conditions in a nuclear waste repository include elevated temperatures as a result of the radioactive decay of the stored waste. Depending on the type of repository and waste form, temperatures up to 200 °C are generally considered. A concise review of literature data on aqueous actinide chemistry up to 90 °C is given by Rao, presenting data on Th(IV), U(VI), Np(V), Am(III) and Cm(III) [7]. The data reviewed contains hydrolysis and complexation reactions with inorganic and small organic ligands. Considering complexation of trivalent actinides with chloride, work perfomed in $CaCl_2$ solutions at 25 °C by Fanghänel et al. and Könnecke et al. give log β°_1 = 0.24 ± 0.03 and log β°_2 = 0.74 ± 0.05 [8,9]. These values were selected for $AnCl^{2+}$ and $AnCl_2^+$ by the NEA TDB database [5]. Yeh et al. report on the formation of $AmCl_n^{(3-n)+}$, giving an increasing log $\beta'_1(t)$ from 0.11 ± 0.05 at 25 °C to 0.38 ± 0.05 at 50 °C in 1 M $NaClO_4$ [10]. No ionic strength corrections have been performed. This gives rise to a positive reaction enthalpy of $\Delta_r H$ = 19.4 ± 7.4 kJ mol $^{-1}$, which in turn contradicts the exothermic estimates of $LnCl^{2+}$ complexes by Choppin et al. and Moulin et al. of about $\Delta_r H$ = 0.21 kJ mol $^{-1}$ [11,12]. Further thermodynamic studies on the complexation of lanthanides with chloride at elevated temperatures will be discussed in Section 3.4 in comparison with the results of this study.

In a previous study on chloride complexation of Cm(III), Skerencak Frech et al. investigated the formation of $CmCl_2^+$ in NaCl in the temperature range from 25 to 200 °C [13]. The authors give a TRLFS based stability constant of log β°_2 = 0.81 ± 0.35 at 25 °C. While spectroscopic evaluation yielded component spectra of $CmCl^{2+}$, $CmCl_2^+$ and $CmCl_3$, the thermodynamics of $CmCl^{2+}$ could

* Corresponding author at: Physikalisch-Chemisches Institut, Ruprecht-Karls-Universität Heidelberg, Im Neuenheimer Feld 253, Heidelberg 69120, Germany.
E-mail address: carsten.koke@partner.kit.edu (C. Koke).

not be evaluated due to very low molar fractions of this complex. This may be considered a consequence of the very limited range of ligand concentration achievable in NaCl with respect to the com plex formation. From this, little variation in emission spectra are obtained, which can lead to an overestimation of the stability constant of $CmCl_2^+$, and an underestimation of $CmCl^{2+}$, accordingly. As a consequence, sound determination of of $CmCl_n^{(3-n)+}$ complex fluorescence spectra benefits from a broader range of spectra, which can be obtained at higher ligand concentrations. To this end, chloride baring electrolytes with high solubility have to be employed, such as LiCl. Also, the use of divalent electrolytes such as $CaCl_2$ increase the ionic strength of the solution, showing similar effects at medium ligand concentrations. While the stability con stant provided by Skerencak Frech et al. can be considered an improvement on previous data, the chloride complexation of Cm (III) is still not thoroughly evaluated for solution conditions in a geochemical setting.

In the present study, time resolved laser fluorescence spec troscopy (TRLFS) in combination with a custom built high temperature cell is applied to study the formation of $CmCl_n^{(3-n)+}$ complexes at t = 25 200 °C in solutions of LiCl, NaCl, $MgCl_2$, and $CaCl_2$. Cm(III) is chosen as a representative for trivalent actinides to determine the thermodynamic data (log $\beta^\circ_n(T)$, $\Delta_r H^\circ$, $\Delta_r S^\circ$, $\Delta_r C^\circ_p$) of $AnCl_n^{(3-n)+}$ complexes at elevated temperatures based on a sizable dataset.

2. Experimental section

Concentrations are given in the temperature independent molal scale (mol (1 kg H_2O) $^{-1}$).

2.1. Chemicals

A stock solution of Cm(III) at b(Cm(III), stock) = 2.12 10^{-5} mol kg $^{-1}$ in perchloric acid was used for sample preparation. The Cm(III) was obtained by ion exchange chromatography from a Cf(III) source, the isotopic mixture was composed of 89.7% ^{248}Cm, 9.4% ^{246}Cm and 0.3% ^{244}Cm, with trace amounts of ^{243}Cm, ^{245}Cm and ^{247}Cm, as determined by inductively coupled plasma mass spectrometry (ICP MS). All chemicals were of analytical grade pur chased through Sigma Aldrich, Alfa Aesar or Merck, and were used without further purification. Table 1 provides an overview of the employed commercial chemical compounds. The samples were prepared by adding the Cm(III) stock solution to solutions with respective amounts of chloride bearing reagents (LiCl, NaCl, $MgCl_2$, $CaCl_2$ 4 H_2O), to achieve a total concentration of b(Cm(III), sample) = 10^{-7} mol kg $^{-1}$. To avoid hydrolysis or sorption to the spectro scopic cell, the conditional pH was kept constant at a proton con centration of $b(H^+)$ = 8.92 10^{-2} mol kg $^{-1}$ by adding HCl for chloride bearing samples, or $HClO_4$ for the Cm(III) aquo ion refer ence. A detailed overview of the measured samples is provided in the Supplementary information.

Table 1
Table of commercial chemical compounds.

Chemical Name	Source	Initial Mole Fraction Purity	Purification Method
hydrochloric acid	Merck	0.9999	none
lithium chloride	Sigma Aldrich	0.9999	none
sodium chloride	Merck	0.9999	none
magnesium chloride	Alfa Aesar	0.9999	none
calcium chloride tetrahydrate	Merck	0.99995	none

2.2. Time resolved laser induced fluorescence spectroscopy (TRLFS)

The measurements were performed in a custom built spectro scopic cell made from Ti/Pd alloy, technical specifications are given elsewhere [14]. The beam of a laser system comprised of a Nd:YAG pulsed laser (Surelite II, Continuum) and a dye laser unit (Narrow Scan, Radiant Dyed Laser & Accessoires) was guided to the cell through a quartz fibre bundle at a repetition rate of 10 Hz. Fluores cence was collected by the same bundle resulting in a detection angle of 180°, guiding the emission light to an optical spectrum analyzer consisting of a polychromator (1200 mm $^{-1}$ grating, Sham rock 303i, ANDOR) and an ICCD camera (iStar Gen III, ANDOR). Cm (III) in solution was excited at a wavelength of 396.6 nm, lumines cence spectra were detected from 570 to 630 nm. To avoid interfer ence of scattering light or short lived luminescence originating from components of the experimental setup, a delay time of 1.5 ms was employed.

Data treatment was performed with OriginPro 2015G (Origi nLab Corp., v. 2015G) and MATLAB (The MathWorks, Inc., v. R2015a). Emission spectra were normalized by total area. Peak deconvolution was performed as a linear combination of single emission bands to fit the total emission spectrum. A baseline cor rection was performed on all spectra necessitated by the invariant background caused by the fibre bundle.

3. Results and discussion

3.1. Emission spectra

For all electrolytes employed, similar spectra have been obtained at comparable sample conditions (e.g. t, I, b(Cl)). This is to be expected, as only ligands in the first coordination shell affect the fluorescence emission of Cm(III). Hence, spectra of the LiCl system will be discussed exemplarily for all systems investi gated, as all significant spectral features occur in this series. Spec tra of each system are given in the SI for comparison. Emission spectra at b(Cl) = 17.9 mol kg $^{-1}$ and t = 25 200 °C are shown in Fig. 1.

A decrease in absolute fluorescence intensity of about 80% with elevation of the temperature is observed independently of the chloride concentration. This effect is partially attributed to

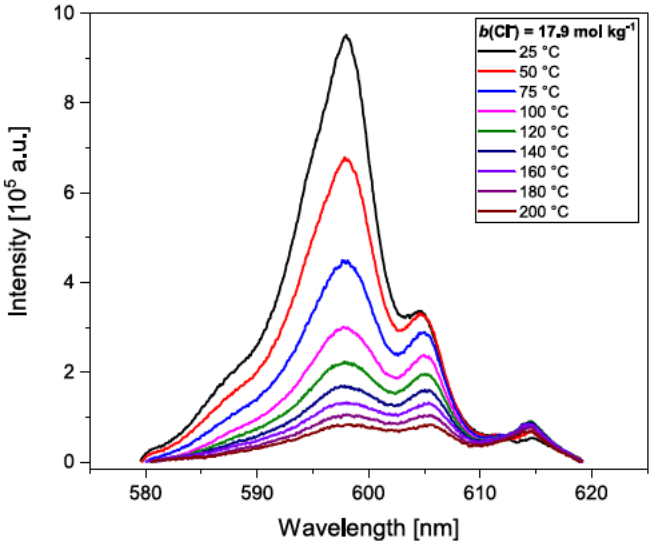

Fig. 1. Emission spectra of Cm(III) in aqueous LiCl solution at t = 25–200 °C (b(Cm (III)) = 10^{-7} mol kg $^{-1}$, b(Cl) = 17.9 mol kg $^{-1}$, $b(H^+)$ = 8.9 · 10^{-2} mol kg $^{-1}$).

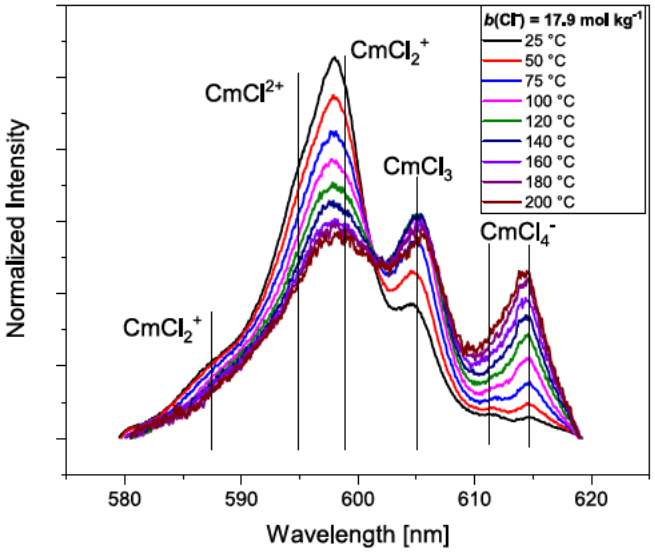

Fig. 2. Normalized emission spectra of Cm(III) in aqueous LiCl solution at t = 25–200 °C (b(Cm(III)) = 10 ^{7} mol kg ^{1}, b(Cl) = 17.9 mol kg ^{1}, b(H^{+}) = 8.9·10 ^{2} mol kg ^{1}).

non radiative de excitation from thermally populated levels [15], while it is also considered to originate from increased quenching through OH vibrational modes of the aquo ligands [14]. Sorption to the cell walls can be largely disregarded at the acidic experimen tal conditions. For further data treatment and discussion, the spec tra are normalized to the total emission intensity as shown in Fig. 2.

The emission shifts to larger wavelengths with increasing chlo ride concentration and elevated temperature. The effect originates from a decrease in energy of the excited state of the Cm(III) ion through an increase of the ligand field splitting. This is a clear indi cation of $CmCl_n^{(3-n)+}$ complex formation. This behavior is also known for the coordination equilibrium of the Cm(III) aquo ion $Cm(H_2O)_{8,9}^{3+}$, where the molar fraction of the octa aquo complex increases with increasing temperature, resulting in a small batho chromic shift [16]. However, this minor effect is negligible com pared to very distinctive emission features that can clearly be attributed to chloride complexation.

3.2. Peak deconvolution

To determine the molar fractions of different Cm(III) complexes, their respective single component spectra are required. The exper imentally observed spectrum is the result of the linear combina tion of those spectra, hence deconvolution of the total emission yields the single component spectra. Subtractive deconvolution starting from the Cm(III) aquo ion $Cm(H_2O)_{8,9}^{3+}$, which has been con sidered a single species for this purpose, yields emission bands of the Cm(III) chloro complexes $CmCl_n^{(3-n)+}$ (n = 1 4). At high signal to noise ratio, a subtractive deconvolution approach is usually sufficient. However, as significant data pretreatment has been per formed and the noise level is fairly high, a line shape based fit is employed. Hence, the resulting pure component spectra have been fitted with a pseudo Voigt line shape, which has been chosen to account for line broadening throughout the dataset. Deconvolution results in one band for $CmCl^{2+}$ (595.0 nm), as well as two bands for $CmCl_2^{+}$ (587.4 nm, 598.5 nm), $CmCl_3$ (576.9 nm, 604.9 nm), and $CmCl_4^{-}$ (611 nm, 614.7 nm), each. Attribution of the hypsochromic satellites to the latter species has been reported in the literature, and the peak positions match the values reported in literature very well [8,13,17]. With increasing temperature, the peak positions remain constant, yet emission bands are slightly broadened through population of thermally excited states. Different sets of single component spectra are used for the deconvolution of the spectra at a given temperature interval (25 50 °C, 75 120 °C, 140 180 °C, 200 °C, respectively). Within these intervals, changes of the band shape are negligible. Two examples of emission spectra and inherent single component spectra at 25 and 200 °C are dis played in Fig. 3. While the intensity of emissions attributed to both $CmCl_3$ and $CmCl_4^{-}$ increases, emission intensity of $CmCl^{2+}$ decreases significantly with increasing temperature. Notably, the ratio of both emission bands of $CmCl_2^{+}$ at 587.4 nm and 598.5 nm is also not constant, but increases with increasing temperature. Further more, the majority of the hypsochromic band of $CmCl_3$ at 577 nm is located outside of the evaluated spectral range, while the contribution of the hypsochromic band of $CmCl_4^{-}$ at 611 nm to the total emission spectrum is very small and only of minor rel evance even in systems of the highest temperature and chloride concentration (see residual component at 611 nm at 200 °C in Fig. 3). Hence, due to their small overall intensity and, consequently, their large systematic error, these two emission

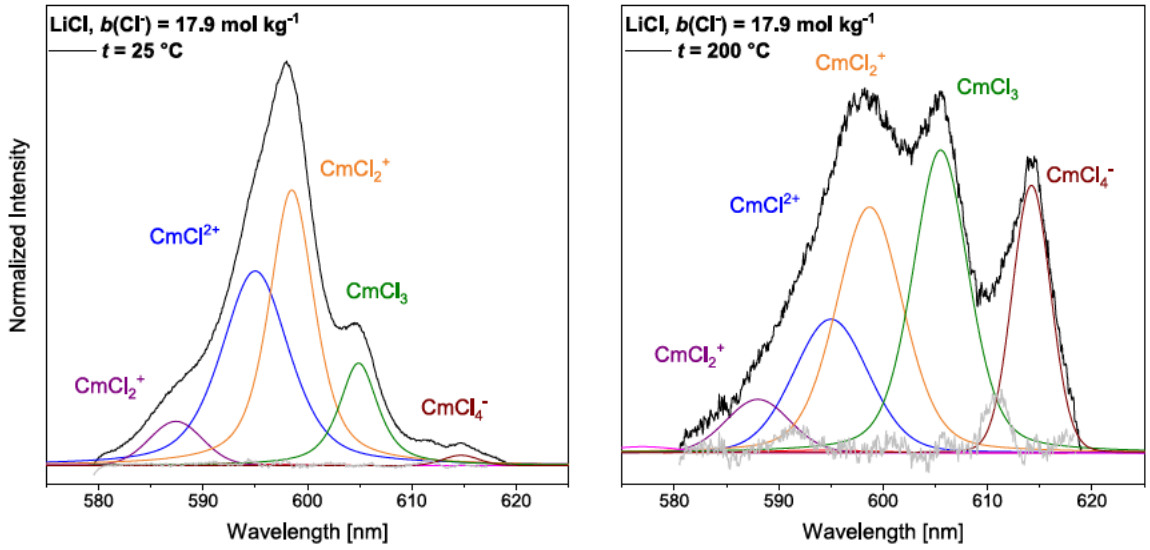

Fig. 3. Single-component spectra of the $CmCl_n^{(3 n)+}$ complexes (n = 1, 2, 3, 4) and examples of peak-deconvoluted emission spectra of Cm(III) at b(Cl) = 17.9 mol kg ^{1}, and t = 25 °C and t = 200 °C, respectively.

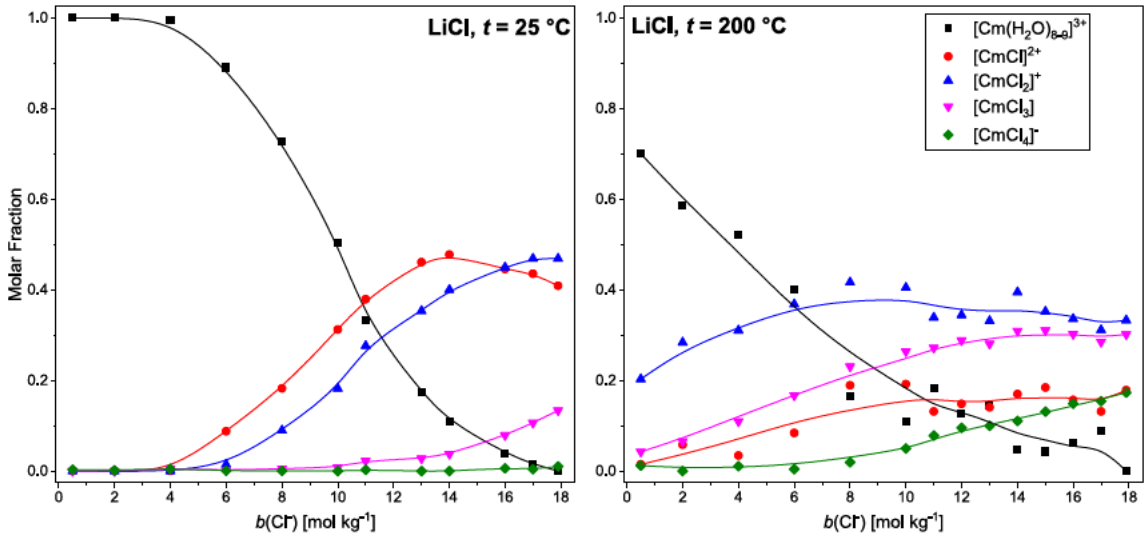

Fig. 4. Molar fractions of the $CmCl_n^{(3-n)+}$ complexes (n = 0–4) as a function of $b(Cl^-)$ at t = 25 and 200 °C.

bands have not been taken into account for spectrum deconvolution.

3.3. Speciation

Relative concentrations of the various Cm(III) species in solution have been derived from the peak areas of the single component spectra determined from the experimental spectra. Fluorescence lifetimes have been found to be strictly monoexponential, while the shape of the emission spectrum does not change even at high delay times. This hints at fast ligand exchange compared to the timescale of fluorescence. Hence, no correction for quantum yield and fluorescence intensity needs to be taken into account [8]. The accuracy of the method is conservatively estimated at 5%. Species distribution diagrams are shown in Fig. 4.

At room temperature and moderate chloride concentrations the Cm(III) aquo ion is the predominant species. At $b(Cl^-)$ > 5 mol kg^{-1} $CmCl_n^{(3-n)+}$ complexes (n = 1–4) occur in significant amounts. A notable feature at room temperature is the formation of $CmCl_2^+$ at very similar conditions as observed for $CmCl^{2+}$. $CmCl_3$ is found at $b(Cl^-)$ > 12 mol kg^{-1}, whereas $CmCl_4^-$ does not occur in any system investigated. At elevated temperatures, larger amounts of Cm(III) chloro complexes are formed, which implies an endothermic reaction for each complex. While $CmCl_3$ makes up a significant molar fraction at 200 °C over the entire concentration range investigated, $CmCl_4^-$ is formed only at both very high temperatures and chloride concentrations above 8 mol kg^{-1}. As can be seen in Fig. 4, the speciation diagrams at elevated temperatures exhibit more data scattering. This is attributed to a lower signal to noise ratio in the recorded spectra.

3.4. Thermodynamics

The conditional stability constant β'_n for the respective Cm(III) chloro complex is calculated according to

$$\beta'_n \quad \frac{\left[CmCl_n^{(3-n)+}\right]}{\left[Cm^{3+}\right] \cdot [Cl^-]^n} \qquad (1)$$

Within the validity range of the *specific ion interaction theory* (SIT), which is employed as the activity model in this study, all electrolytes (HCl, LiCl, NaCl, $MgCl_2$, $CaCl_2$) are assumed to be dissociated [18,19]. Hence, the total chloride concentration is taken to be the free ligand concentration $b(Cl^-)$. While formation of electrolyte complexes (e.g. LiCl (aq), $MgCl^+$, $CaCl^+$) cannot be ruled out at increased electrolyte concentrations, thermodynamic data on the formation of these complexes is hardly available at room temperature, yet completely unavailable at elevated temperatures. Interaction coefficients for ionic strength corrections, if at all documented, are not available for the solution conditions employed in this study. For this reason, a well founded estimation of electrolyte association is not possible, and complete dissociation is assumed for thermodynamic evaluation at all solution conditions.

Minor changes to a single component's intensity result in a change in the calculated stability constant. This fact is of high importance, if the component either dominates the overall spectrum or is present in only minute amounts compared to the overall spectrum. Hence, data of samples with relative species amounts of <5% or >95% has been omitted in the evaluation of thermodynamic data. Values of $\beta'_n(t)$ have been determined for n = 1, 2, 3, 4 in all electrolyte systems investigated at various temperatures. The log $\beta'_n(t)$ show a general trend of increasing values with increasing temperature at constant chloride concentration and ionic strength. At a given temperature, log $\beta'_n(t)$ decreases with increasing ionic strength in the range of I = 0–6 mol kg^{-1}. Fig. 5 shows log β'_2(160 °C) as a function of I for all electrolytes, clearly exhibiting the aforementioned trend.

The obtained values for log $\beta'_n(T)$ have been used to extrapolate to the thermodynamic reference state of infinite dilution (I = 0, γ_i = 1), giving the standard stability constants log $\beta°_n(T)$. Employing the SIT, the log $\beta°_n(T)$ are obtained as

$$\log \beta'_n(T) \quad \log \beta°_n(T) + (\Delta z^2)_n \cdot D(T) \quad \Delta\varepsilon_n(T) \cdot I \qquad (2)$$

The equation takes into account the ion charge coefficient $(\Delta z^2)_n$ = 6, 10, 12, 12, for n = 1, 2, 3, 4, respectively, the summed binary ion interaction parameter $\Delta\varepsilon_n(T) = \Sigma(\varepsilon(i,k,T)_{products}) \quad \Sigma(\varepsilon(i,k,T)_{educts})$ for cation i and anion k, and the Debye Hückel term $D(T) = [A(T)\, I^{0.5}]/[1 + B\alpha_i\, I^{0.5}]$, with A and B being temperature dependent parameters accounting for charge density and ion size. It can clearly be seen in Fig. 5 that the SIT model fits the data very well at $I \leq 6$ mol kg^{-1}, while at higher I the data substantially deviates from the model. This is to be expected, as SIT is limited to low I. Other models like the Pitzer model are more accurate at very high I.

However, there are reasons for using SIT. Firstly, there are hardly any temperature dependent Pitzer parameters for actinides

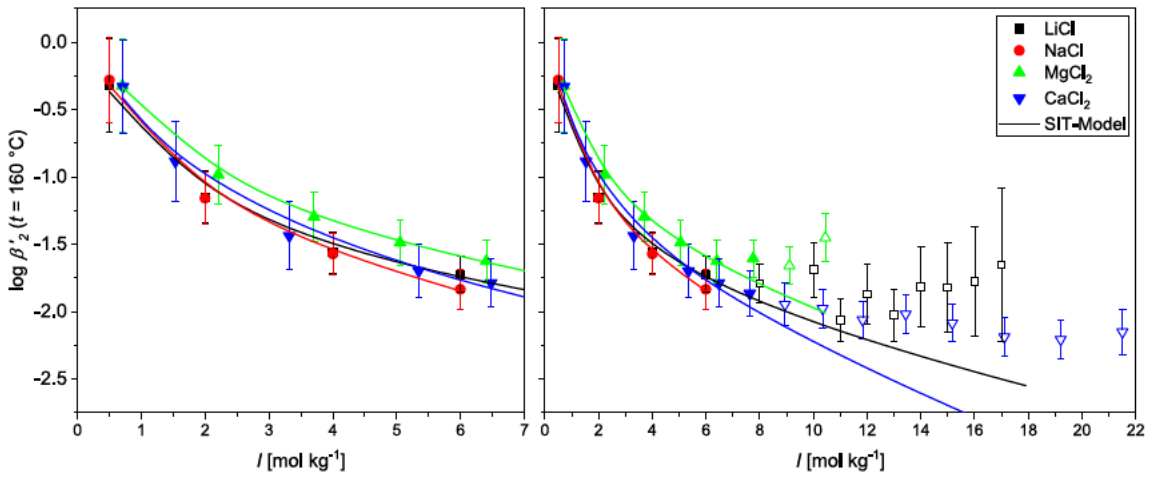

Fig. 5. Stability constants log β'_2(160 °C) as a function of the ionic strength I for all investigated electrolyte systems. Void data points were not considered for extrapolation to the reference state.

available in literature. Secondly, determination of the Pitzer inter action parameter $\beta^{(0)}$ at low ionic strengths is not possible due to insufficient complexation. Furthermore, the SIT model is com monly used within most databases for actinide research in aqueous systems, such as the ThermoChimie and NEA TDB databases [5,20].

As can be seen from Eq. (2), regression analysis of log $\beta'_n(T)$ as a function of I yields both log $\beta^\circ_n(T)$ and $\Delta\varepsilon_n(T)$. Data obtained for $I \leq 6$ mol kg^{-1} has been used in the SIT regression [21]. Determina tion of log $\beta^\circ_2(T)$ in this work is based on a sizable dataset for this particular complex and is shown alongside literature data in Fig. 6. log $\beta^\circ_3(t)$ is evaluated for 180 and 200 °C, while log $\beta^\circ_{1,4}(t)$ are not determined because of very small complex fractions at $I = 0$ 6 mol kg^{-1}. Values for log $\beta^\circ_{2,3}(t)$ in the respective electrolyte solutions are given in the SI.

Extrapolation to reference state temperature of 298.15 K is per formed according to the van't Hoff equation. The integrated van't Hoff equation is

$$\log \beta^\circ_n(T) \quad \log \beta^\circ_n(T_0) + \frac{\Delta_R H^\circ_m(T_0)}{R \ln 10}\left(\frac{1}{T_0} \quad \frac{1}{T}\right) + \frac{\Delta_R C^\circ_{p,m}}{R \ln 10}\left(\frac{T_0}{T} \quad 1 + \ln\frac{T}{T_0}\right) \tag{3}$$

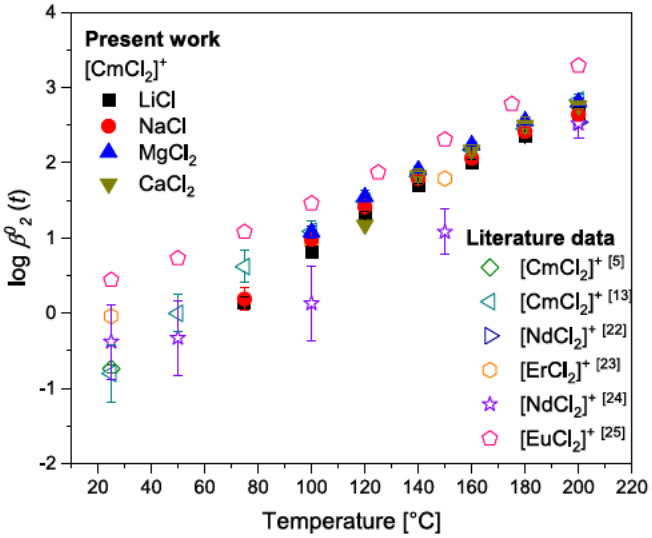

Fig. 6. Stability constants log $\beta^\circ_2(t)$ as a function of temperature for different electrolytes in comparison to literature data.

In case of constant $\Delta_R H^\circ$ (T) over the investigated temperature range a linear relation of log $\beta^\circ_n(T)$ against $1/T$ is apparent and $\Delta_R C^\circ_p \approx 0$. By applying linear regression to log $\beta^\circ_n(T)$ against $1/T$, $\Delta_R H^\circ$ (T_0) and $\Delta_R S^\circ$ are obtained from the regression slope and y axis intersection, respectively.

All individual experimental data for log $\beta^\circ_2(T)$ were weighted by their respective statistical and systematical errors and have been fitted in a single van't Hoff regression, given in the SI. Regarding data consistency within this study it can be seen, that the distribu tion of log $\beta^\circ_2(T)$ values with respect to the electrolyte at a given temperature is very narrow. The equation fits the data with very high accuracy with $R^2 > 0.99$. Hence, no extension accounting for $\Delta_R C^\circ_p$ is needed, yielding the thermodynamic constants and func tions given in Table 2.

Regression on log $\beta^\circ_2(t)$ of separate electrolytes yields different values for log β°_2(25 °C), and the stability constants appear to be slightly, yet systematically dependent on electrolyte valency, as log $\beta^\circ_2(t, \mathrm{M(I)}) <$ log $\beta^\circ_2(t, \mathrm{M(II)})$ (see Table S02). This might origi nate from the SIT model, which does not differentiate between the influence of anions in second shell coordination and anions in the bulk solution. Furthermore, approximating $b(\mathrm{M^+,X^-})$ of elec trolyte MX as I with respect to ion interaction (cf. Eq. (2)) is only valid for monovalent electrolytes. This could give rise to a slight dependence on the electrolyte in very weakly coordinating sys tems. So far, this has not been observed in systems with strong inorganic or organic ligands.

Compared to available literature data, the results of the present work show good agreement with previous studies (see Fig. 6). Pre vious work on temperature dependency of log $\beta^\circ_2(t)$ for $CmCl_2^+$ pre sents slightly larger values at $t \geq 100$ °C, yet they agree well within the margin of error [13]. Data on $NdCl_2^+$ and $ErCl_2^+$ complexes are in good agreement with the present work at $t \geq 100$ °C, however extrapolation to a value of log β°_2(25 °C, $ErCl_2^+$) = 0.04 appears to be an overestimate [22,23]. Another study on $NdCl_2^+$ exhibits

Table 2
Thermodynamic data for the complex formation of $CmCl_2^+$. Stability constant log β°_2(25 °C), reaction enthalpy $\Delta_R H^\circ$ and reaction entropy $\Delta_R S^\circ$ (T) according to the reaction: $Cm^{3+} + 2Cl^- \rightleftarrows CmCl_2^+$.[a]

log β°_2(25 °C)	−1.16 ± 0.10	
$\Delta_R H^\circ$	60.5 ± 1.5	kJ mol^{-1}
$\Delta_R S^\circ$ (T)	180.7 ± 3.9	J mol^{-1} K^{-1}

[a] The confidence intervals provided are given as expanded uncertainties U (0.95 level of confidence).

significantly lower values of log $\beta^\circ_2(t)$ associated with large errors in the temperature range of 100 150 °C, which do not exhibit a van't Hoff behavior [24]. On the contrary, data on the $EuCl_2^+$ complex by Migdisov et al. yields higher values over the complete temperature range investigated [25].

With respect to log β°_2(25 °C), this study shows a notably lower value of 1.16 ± 0.10 compared to values in previous studies on rare earth elements (REE) of 0.42 0.53 for $REECl^{2+}$ [25], and also a slightly lower value compared to 0.74 ± 0.03 or 0.81 ± 0.35 for $CmCl_2^+$ [5,13]. Still, the general increase of the complex stability with increasing temperature is represented well, as can be seen from Fig. 6. This is also represented in the thermodynamic functions of the reaction enthalpy and entropy. The values obtained in this study for $CmCl_2^+$ of $\Delta_R H^\circ = 60.5 \pm 1.5$ J mol $^{-1}$ and $\Delta_R S^\circ(T) = 180.7 \pm 3.9$ J mol $^{-1}$ K $^{-1}$ fit those provided by Skerencak Frech et al. at $\Delta_R H^\circ = 54.9 \pm 4.5$ J mol $^{-1}$ and $\Delta_R S^\circ(T) = 168.8 \pm 5.5$ J mol $^{-1}$ K $^{-1}$ well, considering the limited concentration range of the previous study and inclusion of $\Delta_R C^\circ_p = 40 \pm 10$ J mol $^{-1}$ K $^{-1}$ in their regression [13]. The different thermodynamic functions for Cm(III) and REE(III) chloro complexes in literature can be most likely attributed to previous underestimation of the $CmCl^{2+}$ species, which is hardly observable in the range of I and b(Cl) applied in the previous studies. Trends observed over the entire range of I and b(Cl) in four different electrolytes of this study hint towards a more significant role of this complex at lower temperatures.

4. Conclusion

In the present work a spectroscopic study on the complexation of Cm(III) with chloride in a concentration range of up to 17.9 mol kg $^{-1}$ at temperatures up to 200 °C in different electrolytes was performed. TRFLS spectra show the formation of increasingly coordinated $CmCl_n^{(3-n)+}$ (n = 1 4) complex species with increase of chloride concentrations and temperature, providing evidence for the existence of $CmCl_4$ for the first time. Temperature dependent stability constants were determined and extrapolated to the reference state by SIT. The value for log $\beta^\circ_2(t)$ increases by more than 3 orders of magnitude in the investigated temperature range. Thermodynamic functions $\Delta_r H^\circ$ and $\Delta_r S^\circ$ were evaluated through van't Hoff modeling. It was shown that $\Delta_r C^\circ_p$ is negligible.

This study emphasizes the relevance of actinide geochemistry investigations at elevated temperatures, as supposedly weak complexation reactions at room temperature, such as chloride complexation, are heavily increased in relevance at temperatures above 100 °C. With respect to the nuclear waste disposal safety case, experimental data at room temperature may not yield reliable models for short and medium term repository scenarios.

Conflicts of interest

There are no conflicts to declare.

Acknowledgements

All spectroscopic measurements were carried out at the Institute for Nuclear Waste Disposal (INE) at Karlsruhe Institute of Technology (KIT). This work is supported by the German Federal Ministry of Education and Research (BMBF) under contract 02NUK039C.

Appendix A. Supplementary data

Supplementary data to this article can be found online at https://doi.org/10.1016/j.jct.2018.10.031.

References

[1] International Atomic Energy Agency, Power Reactor Information System, https://www.iaea.org/PRIS/home.aspx, (accessed 26.02.2018, 2018).
[2] International Energy Agency, World Energy Balances 2017, IEA.
[3] International Atomic Energy Agency, Geological Disposal Facilities for Radioactive Waste, International Atomic Energy Agency Y, Vienna, 2011.
[4] International Atomic Energy Agency, Planning and Design Considerations for Geological Repository Programmes of Radioactive Waste, International Atomic Energy Agency, Vienna, 2014.
[5] R. Guillaumont, T. Fanghänel, J. Fuger, I. Grenthe, V. Neck, D.A. Palmer, M.H. Rand, Update on the Chemical Thermodynamics of Uranium, Neptunium, Plutonium, Americium and Technetium, North Holland Elsevier Science Publishers B.V., Amsterdam, The Netherlands, 2003.
[6] T. Thoenen, W. Hummel, U. Berner, E. Curti, The PSI/Nagra Chemical Thermodynamic Database 12/07, Paul Scherrer Institut, Villigen PSI, Switzerland, 2014.
[7] L. Rao, Chem. Soc. Rev. 36 (2007) 881–892.
[8] T. Fanghänel, J.I. Kim, R. Klenze, Y. Kato, J. Alloys Compd. 225 (1995) 308–311.
[9] T. Könnecke, T. Fanghänel, J.I. Kim, Radiochim. Acta (1997) 131–135.
[10] M. Yeh, A.P. Maddison, S.B. Clark, J. Radioanal. Nucl. Chem. 243 (2000) 645–650.
[11] G.R. Choppin, P.J. Unrein, J. Inorg. Nucl. Chem. 25 (1963) 387–393.
[12] N. Moulin, M. Hussonnois, L. Brillard, R. Guillaumont, J. Inorg. Nucl. Chem. 37 (1975) 2521–2524.
[13] A. Skerencak-Frech, D.R. Fröhlich, J. Rothe, K. Dardenne, P.J. Panak, Inorg. Chem. 53 (2014) 1062.
[14] A. Skerencak, P.J. Panak, W. Hauser, V. Neck, R. Klenze, P. Lindqvist-Reis, T. Fanghänel, Radiochim. Acta (2009) 97.
[15] G. Tian, N.M. Edelstein, L. Rao, J. Phys. Chem. A 115 (2011) 1933–1938.
[16] P. Lindqvist-Reis, R. Klenze, G. Schubert, T. Fanghänel, J. Phys. Chem. B 109 (2005) 3077–3083.
[17] M. Arisaka, T. Kimura, R. Nagaishi, Z. Yoshida, J. Alloys Compd. 408–412 (2006) 1307–1311.
[18] E.L. Shock, E.H. Oelkers, J.W. Johnson, D.A. Sverjensky, H.C. Helgeson, J. Chem. Soc., Faraday Trans. 88 (1992) 803–826.
[19] D.A. Palmer, R. Fernandez-Prini, A.H. Harvey, Aqueous Systems at Elevated Temperatures and Pressures, Elsevier Academic Press, London, 2004.
[20] E. Giffaut, M. Grivé, P. Blanc, P. Vieillard, E. Colàs, H. Gailhanou, S. Gaboreau, N. Marty, B. Madé, L. Duro, Appl. Geochem. 49 (2014) 225–236.
[21] M. Altmaier, X. Gaona, T. Fanghanel, Chem. Rev. 113 (2013) 901–943.
[22] A.A. Migdisov, A.E. Williams-Jones, Chem. Geol. 234 (2006) 17–27.
[23] S.A. Stepanchikova, G.R. Kolonin, Russ. J. Coordination Chem. 31 (2005) 193–202.
[24] C.H. Gammons, S.A. Wood, A.E. Williams-Jones, Geochim. Cosmochim. Acta 60 (1996) 4615–4630.
[25] A.A. Migdisov, A.E. Williams-Jones, T. Wagner, Geochim. Cosmochim. Acta 73 (2009) 7087–7109